# Performance Analysis of Fractionalized Order PID Controller-based on Metaheuristic Optimisation Algorithms for Vehicle Cruise Control Systems

Abdelhakim Idir[1,2], Abderrahim Zemmit[1], Khatir Khettab[1], Mokhtar Nesri[3], Sifelislam Guedida[4], Laurent Canale[5]

[1]*Electrical Engineering Department, University of M'sila 28000, Road Bourdj Bou Arreiridj, M'sila 28000 Algeria.*
[2]*Applied Automation Laboratory, F.H.C, University of Boumerdes, 35000 Boumerdes, Algeria.*
[3]*Ecole Supérieur Ali Chabati, Reghaia Algiers, Algeria.*
[4]*Ecole Militaire Polytechnique, UER ELT, 16111 Algiers, Algeria.*
[5]*CNRS, LAPLACE Laboratory, UMR 5213 Toulouse, France.*

## Abstract

Recently, automotive manufacturers have prioritized cruise control systems and controllers, recognizing them as essential components requiring precise and adaptable designs to keep up with technological advancements. The motion of vehicles is inherently complex and variable, leading to significant non-linearity within the cruise control system (CCS). Due to this non-linearity, conventional PID controllers often perform suboptimally under varying conditions. This research introduces a fractionalized-order PID (FrOPID) controller, which has an extra parameter that makes regular PID controllers work better. A comparative analysis is conducted between classical PID controllers and FrOPID controllers optimized using three metaheuristic algorithms: Harris Hawks Optimization (HHO), Genetic Algorithm (GA), and Particle Swarm Optimization (PSO). The evaluation is carried out using a linearized model of the vehicle cruise control system (VCCS). The results demonstrate that fractionalized-order PID controllers significantly outperform conventional PID controllers, particularly regarding rise time and settling time. Among the designs that were considered, the one that combines HHO and FrOPID works the best at finding a balance between responsiveness and stability. It is also the most durable and flexible, able to adapt to changes in vehicle mass and environmental conditions. This highlights the effectiveness of fractionalized-order controllers in managing the dynamic behavior of vehicles.

**Keywords***: Vehicle cruise control system (VCCS), Fractionalized order PID controller, Optimization methods, PID controller, Robustness analysis.*

## 1. Introduction

Reducing fuel usage and emissions of pollutants, especially carbon dioxide and other deleterious compounds, is a considerable challenge for the transportation industry. This dilemma is intensified by global oil constraints and increasing environmental concerns [1]. Automotive manufacturers and authorities have prioritized creative solutions, including new engine technology, smart vehicles, and alternative energy sources [2]. Among these advances, cruise control systems have become a pivotal technology for optimizing fuel efficiency, mitigating driver weariness, decreasing accident risks, and improving traffic flow [3], [4].

Corresponding author: *Abdelhakim Idir (abdelhakim.idir@univ-msila.dz)*
Received: *31 October 2024*; Revised: *6 January 2025*; Accepted: *29 January 2025*; Published: *18 March 2025*

The effectiveness of cruise control systems largely depends on the implementation of proficient control strategies. Proportional-Integral-Derivative (PID) controllers, widely utilized in control engineering, have long been valued for their simplicity, reliability, and robustness. Despite their origins dating back to the 1890s, PID controllers remain integral to approximately ninety percent of industrial processes due to their versatility and ease of implementation [5], [6], [7], [8]. However, their performance in nonlinear and time-varying systems, such as automotive cruise control, is often limited under challenging conditions.

This paper explores the design and optimization of Fractionalized PID (FrOPID) controllers to address these limitations by introducing additional parameters to enhance system performance. The research aims to improve the responsiveness and stability of cruise control systems through metaheuristic optimization techniques, specifically Harris Hawks Optimization (HHO), Genetic Algorithm (GA), and Particle Swarm Optimization (PSO). The study highlights the advantages of FrOPID controllers over conventional PID controllers, particularly in scenarios involving fluctuating vehicle mass and tire friction.

By integrating fractional-order control theory with advanced optimization methods, this study enhances cruise control system performance. Simulations using a linearized vehicle model demonstrate that the proposed FrOPID controllers achieve improved rise time, settling time, and robustness against system uncertainties. Furthermore, this paper evaluates the real-time performance of FrOPID controllers optimized via HHO, GA, and PSO under varying vehicle mass and tire friction conditions. The findings underscore the flexibility and effectiveness of FrOPID controllers in addressing dynamic control challenges, contributing significantly to the advancement of reliable and adaptive cruise control solutions.

The paper is organized as follows: Section 2 presents the literature assessment, Section 3 defines the mathematical modeling of vehicle cruise control systems, and Section 4 examines controller architectures. Section 5 explores metaheuristic optimization techniques, whilst Section 6 presents the proposed fractionalized PID controller optimized via the ITAE criterion. Section 7 presents comparative analyses that validate the superiority of the proposed methods. Section 8 contains the concluding thoughts and recommendations of the paper.

## 2. Literature Review

Recent research has emphasized the advantages of Fractional-Order PID (FOPID) controllers over conventional PID controllers across many applications. FOPID controllers offer superior adaptability in managing systems with nonlinear dynamics and time-dependent parameters. According to Shafiee et al. [9], optimized FOPID controllers outperform conventional PID controllers, particularly in handling complex system dynamics. However, their reliance on simulation results underscores the need for empirical validation. Further evidence supporting the effectiveness of FOPID controllers work comes from experiments conducted by Idir et al. [10] and Mishra et al. [11], demonstrating their robustness in dynamic conditions.

Research on advanced control techniques has demonstrated the effectiveness of fractional PID (Proportional-Integral-Derivative) controllers across various applications. Idir et al. [12] proposed a high-order approximation of a fractional PID controller, optimized using the Grey Wolf Optimization method, specifically for DC motor control. Their study underscored the capability of metaheuristic algorithms to enhance system performance in dynamic environments.

Expanding on these findings, Abualigah et al. [13] proposed a Modified Elite Opposition-Based Artificial Hummingbird Algorithm for designing fractional-order PID (FOPID) controllers in cruise control systems. Their results demonstrated substantial improvements in control precision and system stability using this innovative optimization method. Furthermore, effective control mechanisms have been explored for inherently unstable systems. Bensafia et al. [14] developed a fractional adaptive PID regulator that exhibited enhanced robustness compared to conventional approaches when applied to complex systems. Building on these concepts, Idir et al. [15], [16] investigated the effectiveness of a reduced-order fractional PID controller for aircraft pitch angle regulation and cruise control systems, achieving significant gains in stability and responsiveness.

In contrast to these specific applications, Idir et al. [17] examined the impact of various approximation methods on the design of low-order fractional PID controllers for aircraft systems. Their comprehensive research provided insights into achieving an optimal balance between control complexity and performance. Additionally, Idir et al. [18] conducted a comparative analysis of integer-order PID, fractional-order PID, and fractionalized-order PID controllers on stable systems. This study offered a clear evaluation of the trade-offs and advantages of each control method under varying conditions.

In the automotive sector, the primary objective of cruise control systems is to enhance driver comfort, improve fuel efficiency, and ensure compliance with speed regulations. These systems are critical for maintaining constant vehicle speed while balancing safety, fuel economy, and adaptability. Various control techniques have been explored for this purpose, including traditional PID controllers designed using genetic algorithms, as demonstrated by Rout et al. [19]. To address more complex requirements, PID controllers with reference models, such as those optimized by the improved arithmetic optimization algorithm by Izci et al. [20], have also been developed.

Hlangnamthip et al. [21] optimized PIDA controllers using a Modified Bat Algorithm, demonstrating improved adaptability for vehicle cruise control. Pradhan and Pati [22] proposed an optimal fractional-order PID (FOPID) controller designed to enhance performance in car cruise control systems. Furthermore, innovative approaches, such as ANFIS-based controls combined with fractional-order PD+I controllers, have been validated by Gunasekaran et al. [23], offering a more refined strategy for optimization and flexibility.

Metaheuristic algorithms have proven to be effective tools for optimizing PID and FOPID controllers, particularly in managing the nonlinearities inherent in vehicle cruise control systems. Particle Swarm Optimization (PSO) has been widely applied, as demonstrated by Abdulnabi (2017), who highlighted its ability to enhance system stability and dynamic response [24]. Harris Hawks Optimization (HHO), inspired by the cooperative hunting strategies of Harris hawks, has shown significant effectiveness in improving both PID and FOPID controllers, as evidenced by the research of Izci and Ekinci [25]. Similarly, the Genetic Algorithm (GA), rooted in natural evolutionary principles, has been successfully applied to optimize cruise control systems [26]. Despite these advances, there is limited research on the real-time application of these algorithms in automotive systems, representing a critical gap in the literature.

Emerging optimization algorithms, such as the Red Panda Optimization (RPO) [27], Ant Lion Optimizer (ALO) [28], and Gorilla Troops Optimization (GTO) [29], have also demonstrated their potential in optimizing PID controllers. However, comparative studies on these algorithms remain sparse, particularly concerning their adaptability and performance in real-world scenarios. Advanced algorithms like the Grey Wolf Optimizer and Artificial Bee Colony warrant further exploration, as do studies addressing the trade-offs between safety, fuel efficiency, and adaptability in control strategies.

## 3. Vehicle Cruise Control System (VCCS)

The cruise control systems face challenges in maintaining driver-set speed due to inclines and wind resistance, which can be disrupted by gravitational forces and wind resistance, as illustrated in a schematic diagram given in Figure 1.

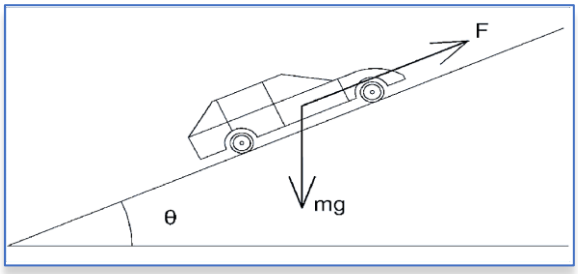


**Figure 1.** VCCS Model.

A vehicle cruise control system regulates the vehicle's velocity by using a predetermined speed as a reference. ($v_{ref}$). Consequently, the vehicle's velocity ($v$) is sustained by adjusting the engine throttle input ($u$). The linearized model that establishes the relationship between the output velocity ($V$) and the control input ($U$) can be derived as follows [9]:

$$G(s) = \frac{\Delta V(s)}{\Delta U(s)} = \frac{\frac{C_1 e^{-\tau s}}{MT}}{\left(s + \frac{2C_a v}{M}\right)\left(s + \frac{1}{T}\right)} \quad (1)$$

where $C_1$ and $C_a$ represent the actuator constant and aerodynamic drag coefficient, respectively, whereas $\tau$ and $T$ are the driver's reaction and observation times, respectively. The vehicle mass is represented by $M$.

Table 1 lists the factors and numbers for the vehicle cruise system simulated in this paper [9], [10].

**Table 1.** VCCS parameters.

| Parameter | Value |
|---|---|
| $C_1$ | 743 |
| $C_a$ | 1.19 N/(m/s)$^2$ |
| $M$ | 1500 $Kg$ |
| $\tau$ | 0.2 $s$ |
| $T$ | 1 $s$ |
| $F_{dmax}$ | 3500 $N$ |
| $F_{dmin}$ | −3500 $N$ |
| $g$ | 9.81 $m/s^2$ |

Given the operating point $v = 30\ km/h$ and referring to Table 1, we can determine the the plant transfer function $G(s)$.

$$G(s) = \frac{\Delta V(s)}{\Delta U(s)} = \frac{2.4767}{(s + 0.0476)(s + 1)(s + 5)} \quad (2)$$

## 4. Controllers Design

### 4.1. Proportional Integral Derivative (PID) controller

Traditional PID controllers are widely used in process industries due to their straightforward design, robustness, and easily comprehensible regulatory processes. Despite the fluctuating dynamic behavior of process plants, conventional PID controllers can deliver excellent control performance.

The classical transfer function of a PID controller is represented by equation (3).

$$G_c(s) = K_p + K_i s^{-1} + K_d s \quad (3)$$

Where $K_p$, $K_i$ and $K_d$, represent the proportional, integral, and derivative gains, respectively.

Then,

$$G_{IOPID}(s) = K_p(1 + \frac{1}{T_i s} + T_d s) \quad (4)$$

Where

$T_i$ : represents the integral time constant

$T_d$: represents the derivative time constant.

### 4.2. Fractionalized Order PID controller

The transfer function of a traditional PID controller is represented by the following equation:

$$G_c(s) = K_p\left(1 + \frac{1}{T_i s} + T_d s\right) \quad (5)$$

The introduction of fractionalisation in the control system component modifies the PID control rule, leading to the fractionalisation of the integral operator $1/s$ [15],[18],[30]:

$$\frac{1}{s} = \frac{1}{s^\alpha} \cdot \frac{1}{s^{1-\alpha}} \quad (6)$$

The fractionalized PID controller to be developed is represented by [15],[31]:

$$G_c(s) = K_p\left(1 + \frac{1}{T_i s} + T_d s\right) = \frac{1}{s}\left(\frac{K_p T_i T_d s^2 + K_p T_i s + K_p}{T_i}\right)$$
$$= \frac{1}{s^\alpha s^{1-\alpha}}\left(\frac{K_p T_d s^2 + K_p T_i s + K_p}{T_i}\right) \quad (7)$$

Where, $0 < \alpha < 1$.

## 5. Metaheuristic Optimisation Algorithms

This section provides a concise summary of the heuristic methods proposed for classical PID and fractionalized order PID.

### 5.1. Harris Hawks Optimization (HHO) algorithm

The HHO algorithm is inspired predatory behavior of Harris hawks. These hawks exhibit cooperative and surprise-based tactics to capture prey, mimicking various dynamic chasing strategies. The HHO algorithm uses these strategies to find an optimal solution to a problem. Below the different steps of the HHO algorithm:

**Step 1:** Initialization;

**Objective:** Define the objective function $f(x)$ to be minimized (or maximized).

**Initialize population:** Generate an initial population of $N$ hawks randomly within the defined search space. Each hawk represents a candidate solution and is denoted as $x_i$, where $i = 1, 2, \ldots, N$.

Set parameters: Define the maximum number of iterations (MaxIter) and other relevant parameters like the number of hawks and search space bounds.

**Step 2:** Evaluate Fitness;
Evaluate the fitness of each hawk based on the objective function $f(x)$. The best fitness among all hawks represents the current best position of the prey, denoted as $X_{\text{rabbit}}$ .

**Step 3:** Hunting Strategies Based on Energy $E$;
Escape energy of prey $E$: The energy of the prey decreases as iterations progress, defined as:

$$E = 2E_0\left(1 - \frac{t}{T}\right) \quad (8)$$

where $E_0$ is a random number between $-1$ and 1, t is the current iteration, and $T$ is the maximum number of iterations. The value of $E$ decides the type of hunting strategy.

**Step 4:** Update Hawks' Positions;
The hawks perform different movements based on the energy $E$. There are two main cases:

***Case 1:*** $|E| >= 1$ (Exploration phase)
When the prey is energetic and still escaping, the hawks explore the search space using random movements. In this phase, the hawks' positions are updated as:

$$X(t+1) = \begin{cases} X_{\text{rand}}(t) - r_1|X_{\text{rand}}(t) - 2r_2X(t)| & q \geq 0.5 \\ X_{\text{rabit}}(t) - X_m(t) - r_3\left(L_b + r_4(U_b - L_b)\right) & q < 0.5 \end{cases} \quad (9)$$

where $X(t+1)$ represents the Hawks' position in the subsequent iteration, $X_{\text{rabbit}}(t)$ indicates the rabbit's position, $X(t)$ denotes the vector indicating the current position of the hawks, $(r_1, r_2, r_3, r_4)$ denote random numbers within the range of(0,1), and $(L_b, U_b)$ represent the variables of lower and upper bounds.

***Case 2:*** $|E| < 1$ (Exploitation phase)

The final phase of the HHO algorithm consists of four distinct strategies, each contingent upon the energy level of the prey and the likelihood of its escape. When considering $r < 0.5$ as indicative of the prey's successful escape chance and $r \geqslant 0.5$ as representing an unsuccessful escape attempt: - In cases where $r \geqslant 0.5$ and $|E| \geq 0.5$, a soft besiege strategy will be executed, characterized by Equations (10) and (11).

$$X(t+1) = \Delta X(t) - E|JX_{\text{rabbit}}(t) - X(t)|, \quad (10)$$

$$\Delta X(t) = X_{\text{rabbit}}(t) - X(t), \quad (11)$$

where ΔX(t) represents the disparity between rabbit's location and current location at iteration $t$, while $J$ denotes the magnitude of the rabbit's random jump.

- For $r \geqslant 0.5$ and $|E \leq 0.5|$, A severe besiege will be undertaken, as stated by Eq.(12).

$$X(t+1)X_{\text{rabbit}} - E|\Delta X(t)| \quad (12)$$

For $r < 0.5$ and $|E| \geq 0.5$, A mild besiege with gradual quick drive will be executed, as stated by Eqs.(13) and (14).

$$Y_1 = X_{\text{rabbit}} - E|JX_{\text{rabbit}} - X(t)|, \quad (13)$$

$$Z_1 = Y_1 + S \times LF(D), \quad (14)$$

where $D$ is the dimension of the problem, $S$ is a $1xD$ random vector, and LF is the levy flight function.

Therefore, Eq. (15) fulfills the position update.

$$X(t+1) = \begin{cases} Y_1, & \text{if } F(Y_1) < F\big(X(t)\big) \\ Z_1, & \text{if } F(Z_1) < F\big(X(t)\big) \end{cases} \quad (15)$$

- If both $r$ and $|E|$ have values lower than a certain threshold, a hard besiege with increasing quick drive will be used, as described by Equations (16)-(18).

$$X(t+1) = \begin{cases} Y_2, & \text{if } F(Y_2) < F\big(X(t)\big) \\ Z_2, & \text{if } F(Z_2) < F\big(X(t)\big) \end{cases} \quad (16)$$

$Y_2$ and $Z_2$ are obtained using (17) and (18), respectively.

$$Y_2 = X_{\text{rabbit}} - E|JX_{\text{rabbit}} - X(t)|, \quad (17)$$

$$Z_2 = Y_2 + S \times LF(D). \quad (18)$$

**Step 5:** Evaluate New Solutions;
Evaluate the fitness of each hawk after updating their positions. If a hawk's new position provides a better solution, update the current best position. $X_{\text{rabbit}}$ .

**Step 6:** Check Stopping Criterion;
If the maximum number of iterations MaxIter is reached or the desired solution is found, stop the algorithm.

**Step 7:** Return the Best Solution
Return the position $X_{\text{rabbit}}$ as the optimal solution found by the algorithm.

For illustration, the overall flowchart of the HHO algorithm is presented in Figure. 2.

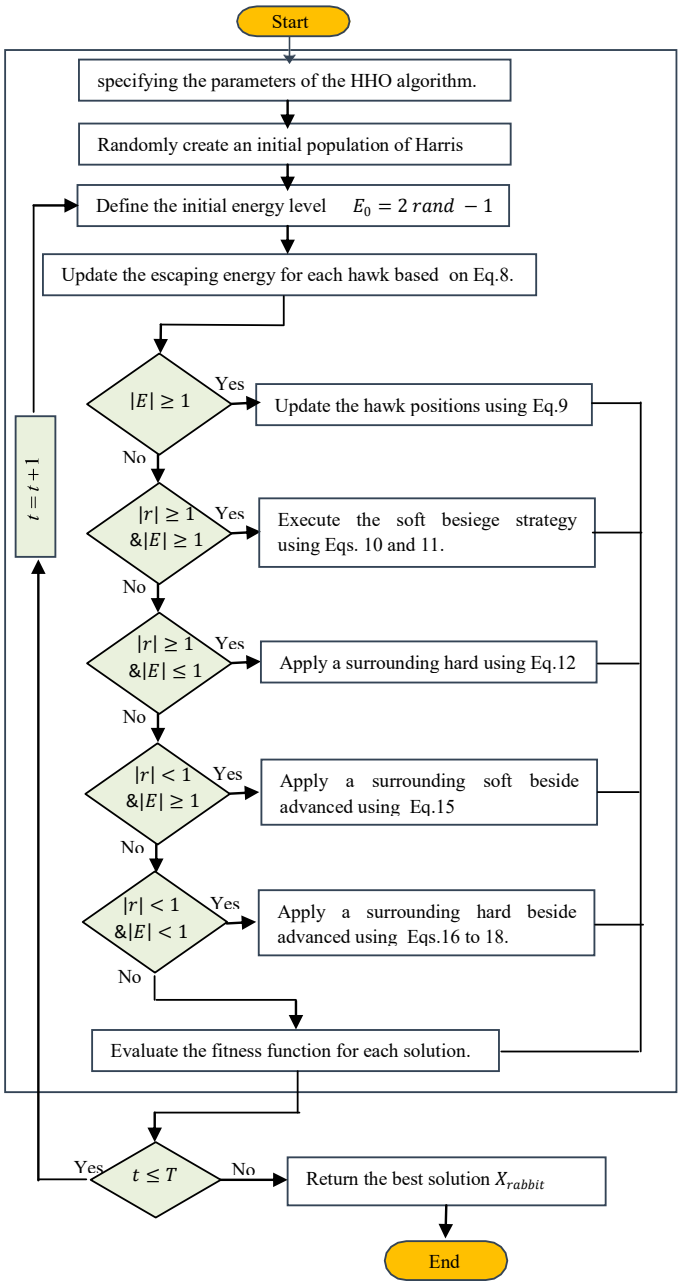


**Figure 2.** Flowchart of the HHO algorithm.

### 5.2. Genetic Algorithm (GA)

The GA is a bio-inspired optimization technique based on the principles of natural selection and genetics. It aims to find the optimal solution to a problem by evolving a population of candidate solutions over several generations. Below is a detailed explanation of each step:

**Step 1:** Initialization;

- ***Objective***: Define the objective function $f(x)$ to be optimized.
- ***Generate the initial population***: Create an initial population of $N$ individuals (candidate solutions), each represented by a chromosome (a set of encoded parameters). The chromosome can be a binary string, real numbers, or any other representation suitable for the problem.
- **Set parameters**: Define the population size $(N)$, number of generations $(MaxGen)$, crossover probability $(p_c)$, mutation probability $(p_m)$, and other relevant parameters.

**Step 2:** Evaluate Fitness;

Examine the fitness of each member within the population via the objective function $f(x)$.

- The fitness value signifies the quality of each potential solution.

**Step 3:** Selection;

- Select parent individuals from the current population based on their fitness. This process is usually stochastic, with better solutions having a higher chance of being selected.

**Step 4:** Crossover (Recombination);

- Perform crossover between selected parent individuals to generate new offspring (children).

**Step 5:** Mutation;

- Implement mutation in offspring with a specified probability. Mutations assist to preserve genetic variety and avoid premature convergence by introducing random modifications to particular genes inside the chromosome.

**Step 6:** Evaluate New Population;

- Calculate the fitness of the new offspring population.
- Combine the offspring with the current population if needed, depending on the chosen GA strategy.

**Step 7:** Replacement;

- Select individuals for the next generation based on fitness.

**Step 8:** Check Stopping Criterion;

- If the maximum number of generations $(MaxGen)$ is reached or if the improvement in fitness is below a certain threshold, stop the algorithm.

**Step 9:** Return the Best Solution.

Return the best individual from the final population as the optimal solution.

### 5.3. Particle Swarm Optimization (PSO) algorithm

The PSO algorithm is a widely utilized optimization method derived from the social behaviors shown by birds in flocks or fish in schools. It identifies the ideal answer by progressively enhancing a population of possible solutions referred to as particles. These particles explore the search space by updating their positions and velocities according to their own experiences and those of their neighbours.

Below is a detailed sequential analysis of the PSO algorithm:

**Step 1:** Initialization;

Objective: Define the objective function $f(x)$ to be minimized (or maximized). Randomly initialize the position and velocity of each particle within the search space. Each particle $i$ has a position $x_i$ and velocity $v_i$. Set parameters such as the number of particles $N$, maximum iterations (MaxIter), inertia weight $(w)$, cognitive coefficient $(c_1)$, and social coefficient $(c_2)$.

**Step 2:** Fitness evaluation;

Evaluate the fitness of each particle using the objective function $f(x)$. Identify the personal best position $(pbest_i)$ for each particle and the global best position $(gbest_i)$ among all particles.

**Step 3:** Velocities updating;

Update the velocity of each particle using the equation:

$$v_i^{k+1} = w_i v_i^k + c_1 r_1 \left(pbest_i - x_i^k\right) + c_2 r_2 \left(gbest_i - x_i^k\right) \quad (19)$$

where $r_1$ and $r_2$ are random values between 0 and 1. $w_i$ is the inertia weight that controls the influence of the previous velocity. While $c_1$ and $c_2$ are cognitive and social coefficient respectively.

**Step 4:** Positions updating;

Update the position of each particle using the equation:

$$x_i^{k+1} = x_i^k + v_i^{k+1} \quad (20)$$

**Step 5:** New fitness evaluation;

- Evaluate the fitness of each particle at its updated position.
- If a particle's new position yields a better fitness, update its personal best $(pbest_i)$.
- Update the global best $(gbest)$ if necessary.

**Step 6:** Evaluation of the stopping criteria;

Stop the algorithm if the maximum number of iterations is reached or the change in fitness values is below a predefined threshold.

**Step 7:** Return the Best Solution.

Return the global best position $(gbest)$ as the optimal solution.

## 6. Proposed Design Procedure and FrOPID Controlled VCCS

Figure 3 describes a vehicle cruise control system using a PID and FrOPID feedback loop. In this system, $G(s)$ and $G_{FrOPID}(s)$ represent the plant and controller models, respectively.

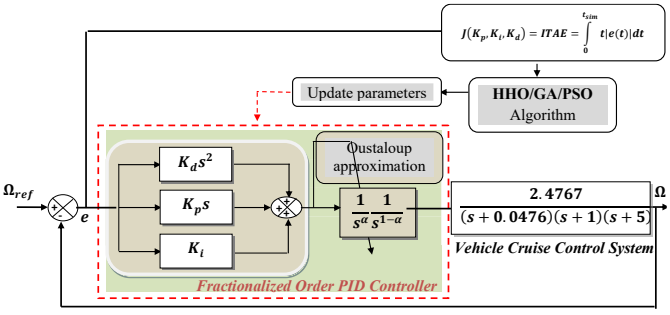


**Figure 3.** Proposed HHO/GA/PSO based FrOPID Controller.

The models apply the ITAE objective function to enhance key performance indicators. The controller manages the output Ω (speed), based on the input $\Omega_{ref}$ (reference speed), ensuring that the system remains stable and performs as desired, even in the presence of external disturbances $D(s)$.

The design of a traditional PID controller is represented by equation 4 as discribed in section 4.1, where:

$$G_{PID}(s) = K_p\left(1 + \frac{1}{T_i s} + T_d s\right) \quad (21)$$

The enhancement of classical PID controller is represented by equation 22 as discribed in section 3.2,

$$G_{FrOPID}(s) = \frac{1}{s^{\alpha} s^{1-\alpha}}\left(\frac{K_p T_i T_d s^2 + K_p T_i s + K_p}{T_i}\right) \quad (22)$$

Where, $0 < \alpha < 1$.

This study uses ITAE as the performance criterion for various optimization methods, where the error e(t)e(t) represents the difference between the reference model and the actual model. Smaller error values signify better alignment with the desired controller parameters.

$$J(K_p, K_i, K_d) = ITAE = \int_0^{t_{sim}} t|e(t)|dt \quad (23)$$

The letter $J$ denotes the performance criteria, indicating the degree of resemblance between the controlled object and the reference model, while $e(t)$ represents the error signal. Here, $e(t)$ corresponds to the disparity between the reference speed and the actual speed $(v_{ref}(t) - v(t))$. The simulation time $(t_{sim})$ was set to 10 seconds for this investigation.

## 7. Numerical Simulation Results and Discussion

This section presents the simulation results of the proposed architecture, which is based on the linearizing feedback and the FPID controller. The simulation process was carried out using MATLAB, a powerful tool for modeling and simulating control systems. Table 2 lists the parameters of the proposed HHO, GA and PSO algorithms.

The classical PID and the proposed Fractionalized Order PID (FrOPID) controllers for vehicle cruise control are optimized by three metaheuristic algorithms—Harris Hawks Optimization (HHO), Genetic Algorithm (GA), and Particle Swarm Optimization (PSO). The controller's performance is compared against that of a classical PID controller optimized by various contemporary methodologies.

The unity feedback closed-loop transfer function of the fractionalized-order PID controller, optimized using HHO, GA, and PSO algorithms, incorporates an integrator with a fractional order $\alpha = 0.5$. This fractional order is approximated using the Oustaloup technique. The approximation parameters are: are $\omega_b = 0.01$ rad/ s, $\omega_h = 1000$ rad/s and $N = 5$ (filter order).

**Table 2.** Optimization parameters for HHO, GA, and PSO algorithms.

| Algorithm | Parameter | Value |
|---|---|---|
| **HHO** | Population Size | 50 |
| | Maximum Iterations | 40 |
| | Lower bounds $[K_p, K_i, K_d]$ | [0.01;0.0 |
| | Upper bounds $[K_p, K_i, K_d]$ | [5;5; 5] |
| | Time of simulation | 5s |
| **GA** | Population Size | 40 |
| | Crossover Probability | 0.8 |
| | Mutation Probability | 0.125 |
| | Maximum Iterations | 25 |
| | Lower bounds $[K_p, K_i, K_d]$ | [0.01;0.0 |
| | Upper bounds $[K_p, K_i, K_d]$ | [5;5; 5] |
| | Time of simulation | 5s |
| **PSO** | Population Size | 50 |
| | Maximum Iterations | 40 |
| | Acceleration Constants (c1,c2) | 2 |
| | Lower bounds $[K_p, K_i, K_d]$ | [0.01;0.0 |
| | Upper bounds $[K_p, K_i, K_d]$ | [5;5; 5] |

The parameters and corresponding values for these approaches are detailed in Table 3.

**Table 3.** Proposed controller's gain parameters and other controllers compared.

| Controllers | $K_p$ | $K_i$ | $K_d$ | $\alpha$ |
|---|---|---|---|---|
| HHO/FrOPID [Proposed] | 4.1132 | 0.1714 | 4.2564 | 0.5 |
| GA/FrOPID [Proposed] | 3.5907 | 0.1630 | 3.3021 | 0.5 |
| PSO/FrOPID [Proposed] | 3.9578 | 0.1798 | 3.8583 | 0.5 |
| HHO/PID | 4.1132 | 0.1714 | 4.2564 | 1 |
| GA/PID | 3.5907 | 0.1630 | 3.3021 | 1 |
| PSO/PID | 3.9578 | 0.1798 | 3.8583 | 1 |

### 7.1. Transient and frequency stability analysis

Figure 4 presents a comparison of step responses among different controllers, focusing on their performance over time. It includes proposed

fractionalized-order PID (FrOPID) controllers optimized using three metaheuristic algorithms—Harris Hawks Optimization (HHO), Genetic Algorithm (GA), and Particle Swarm Optimization (PSO)—as well as traditional integer-order PID controllers optimized with the same algorithms.

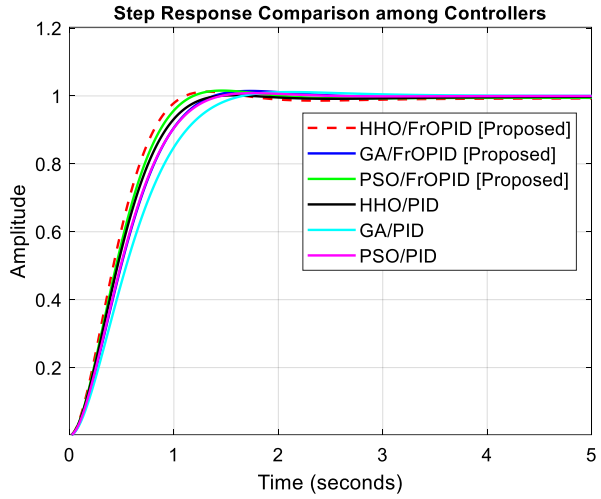


**Figure 4.** Step response of various optimizer-based controller schemes for ACCS.

As can be seen from Figure 4, the results show that the proposed FrOPID controllers consistently outperform their traditional counterparts. Specifically, the HHO/FrOPID controller, represented by a red dashed line, achieves a faster rise to the target value and settles more quickly, indicating a better response with minimal overshoot. This suggests a higher level of control stability and responsiveness. Meanwhile, the GA/FrOPID and PSO/FrOPID controllers also demonstrate improvements, though their rise and settling times are slightly longer compared to the HHO/FrOPID configuration.

In contrast, the traditional PID controllers, represented by solid lines, exhibit slower rise times and more pronounced overshoots. This comparison highlights the effectiveness of using fractionalized-order controllers optimized with advanced algorithms, particularly HHO, to enhance system performance. Overall, the HHO/FrOPID combination proves to be the most efficient in achieving a balance between responsiveness and stability, showcasing the robustness and adaptability of fractionalized PID controllers in dynamic environments.

Figure 5 presents a Bode plot comparison between proposed fractionalized-order PID (FrOPID) controllers and traditional PID controllers, each optimized using Harris Hawks Optimization (HHO), Genetic Algorithm (GA), and Particle Swarm Optimization (PSO). The Bode plot consists of two subplots: one showing the system's magnitude response (in dB) across a range of frequencies, and the other depicting the corresponding phase response (in degrees).

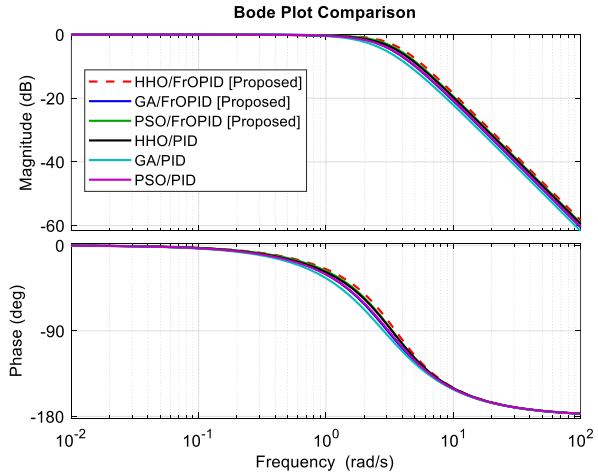


**Figure 5.** Bod plots of various optimizer-based controller schemes for VCCS.

The magnitude graph indicates that the proposed FrOPID controllers exhibit higher gain at lower frequencies, with a more gradual decline as frequency increases. The HHO/FrOPID controller maintains the most consistent gain response across the frequency spectrum, demonstrating improved stability against low-frequency perturbations. In contrast, conventional PID controllers show a more pronounced reduction in magnitude at higher frequencies, indicating reduced effectiveness in maintaining stability across different frequency ranges.

The phase plot indicates that the proposed controllers exhibit a more gradual and consistent phase transition across the frequency spectrum. The HHO/FrOPID controller shows minimal phase deviations, suggesting enhanced overall stability and improved response to dynamic system variations. In contrast, conventional PID controllers experience more pronounced phase reductions at specific frequencies, highlighting increased susceptibility to disturbances and reduced frequency stability.

The results show that the suggested fractional-order PID controllers work better and more reliably across a wide frequency range, making them better than regular PID controllers. When the HHO algorithm is used to improve fractional-order systems, the uniformity in amplitude and phase responses shows how strong and flexible they are. The comparison confirms that fractional-order controllers excel in managing system dynamics and uncertainties, with the HHO/FrOPID configuration demonstrating distinct advantages.

To demonstrate the enhanced efficacy of the suggested technique, we have provided comparative numerical data for the VCCS in both the transient and frequency domains. The results are shown in Tables 4 and 5.

**Table 4.** Performance comparison of transient responses.

| Controllers | $T_r(s)$ | $T_s(s)$ | $OS$ (%) |
|---|---|---|---|
| HHO/FrOPID [Proposed] | 0.65467 | 0.98394 | 1.8203 |
| GA/FrOPID [Proposed] | 0.80665 | 1.8292 | 2.0597 |
| PSO/FrOPID [Proposed] | 0.70573 | 1.5615 | 2.1153 |
| HHO/PID | 0.76319 | 1. 1962 | 0.17565 |
| GA/PID | 0.93938 | 1. 4559 | 1. 1456 |
| PSO/PID | 0.82074 | 1.272 | 0.82093 |

**Table 5.** Performance comparison of frequency responses.

| Controllers | $G_m(dB)$ | $\varphi_m(°)$ | $B_w(Hz)$ |
|---|---|---|---|
| HHO/FrOPID [Proposed] | Inf | Inf | 3.3323 |
| GA/FrOPID [Proposed] | Inf | Inf | 2.6398 |
| PSO/FrOPID [Proposed] | Inf | Inf | 3.0549 |
| HHO/PID | Inf | -180 | 2.8663 |
| GA/PID | Inf | -180 | 2.2657 |
| PSO/PID | Inf | -180 | 2.6264 |

Table 4 compares the transient response metrics; rise time ($T_r$), settling time ($T_s$), and overshoot ($OS\%$) for different controller types, specifically fractionalized-order PID controllers (FrOPID) optimized by HHO, GA, and PSO, and traditional PID controllers. While Table 5 presents frequency response metrics; gain margin ($G_m$), phase margin ($\varphi_m$), and bandwidth ($B_W$) across the same set of controllers.

As can be seen from Tables 4 and 5, the fractionalized order PID controllers (especially HHO/FrOPID) outperform traditional PID controllers in both transient and frequency responses, demonstrating faster rise times and higher bandwidth. This suggests that fractionalized-order controllers are better suited for systems requiring both fast response and high stability, while traditional PID controllers may still be preferable in applications where minimizing overshoot is critical.

Table 6 effectively compares three controllers (HHO/FrOPID, GA/FrOPID, and PSO/FrOPID) across different performance criteria (rise time, settling time, and overshoot) for integrator orders ($\alpha$) ranging from $0.1$ to $0.5$.

**Table 6.** Comparative transient response results for different controllers and integrator orders $\alpha$).

| Criterion | $\alpha$ | HHO/FrOPID | GA/FrOPID | PSO/FrOPID |
|---|---|---|---|---|
| Rise time [s] | 0.1 | 0.71961 | 0.88694 | 0.77530 |
| | 0.2 | 0.69029 | 0.85087 | 0.74403 |
| | 0.3 | 0.67029 | 0.82609 | 0.72225 |
| | 0.4 | 0.65845 | 0.81144 | 0.70992 |
| | 0.5 | 0.65467 | 1.45590 | 1.14560 |
| Settling time [s] | 0.1 | 1.10620 | 1.36030 | 1.18530 |
| | 0.2 | 1.04970 | 1.29520 | 1.12750 |
| | 0.3 | 1.01240 | 1.25100 | 1.08880 |
| | 0.4 | 0.99079 | 1.79260 | 1.53930 |
| | 0.5 | 0.98394 | 1.82920 | 1.56150 |
| Overshoot [%] | 0.1 | 0.76674 | 1.43020 | 1.24420 |
| | 0.2 | 1.20670 | 1.68500 | 1.60290 |
| | 0.3 | 1.54050 | 1.88570 | 1.87980 |
| | 0.4 | 1.75130 | 2.01520 | 2.05500 |
| | 0.5 | 1.82030 | 2.05970 | 2.11530 |

As can be seen from table 6, the The HHO/FrOPID demonstrates the lowest rising time and settling time, signifying a more rapid reaction in comparison to the GA/FrOPID and PSO/FrOPID. Nonetheless, GA/FrOPID demonstrates elevated overshoot values, perhaps resulting in diminished stability. PSO/FrOPID achieves a compromise between rising time and overshoot; nonetheless, it is generally surpassed by HHO/FrOPID in most instances. These results underscore the efficacy of HHO/FrOPID for applications necessitating both rapidity and stability.

### 7.2. Robustness analysis

#### *7.2.1. Effect of changing vehicle mass*

In this subsection, parameter variations are introduced by adjusting the vehicle mass to simulate the effects of fuel consumption. The transfer functions are updated based on the new vehicle mass, and both the nominal and varied-mass systems are compared using step responses and transient response analysis.

Figure 6 shows the comparison between nominal vehicle mass and varied vehicle mass for six different controller types, including both traditional PID and fractionaliazed order PID controllers optimized by HHO, GA, and PSO. The nominal mass system responses are represented by dashed lines while the systems with varied mass are shown in solid lines.

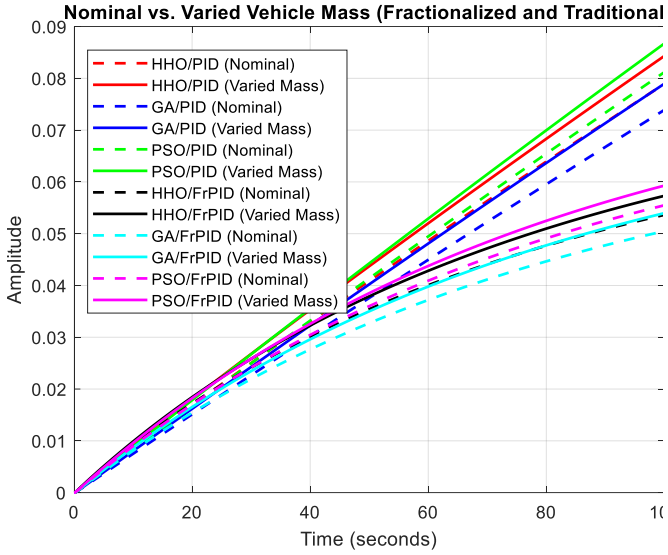


**Figure 6.** Comparison between nominal vehicle mass and varied vehicle mass.

Figure 6 shows that all controllers exhibit a similar rising pattern, with fractional-order PID controllers (FrOPID) achieving faster rise times compared to traditional PID controllers. As shown in Figure 6, the fractional-order versions of the controllers demonstrate slightly better performance, with faster rise and settling times than their traditional PID counterparts, indicating improved handling of parameter variations, such as mass changes.

Table 7 presents the transient response metrics (RiseTime ($T_r$), SettlingTime ($T_s$), Overshoot (OS)) for nominal versus varied vehicle mass, clearly illustrating the controllers' performance under both conditions.

- **For Rise Time**: Fractionalized Order PID controllers achieve significantly faster rise times, around 175-178 seconds, compared to traditional PID controllers, which exceed 2400 seconds for varied mass. The HHO/FrOPID controller, with a rise time of 175.46 seconds for varied mass, stands out as the fastest among all controllers.

- **For Settling Time**: Similarly, fractional PID controllers settle much quicker, within the range of 313-318 seconds, while traditional PID controllers require over 4000 seconds to settle. Once again, HHO/FrOPID exhibits the best settling time performance.

- **For Overshoot:** All controllers demonstrate zero overshoot, indicating stable performance without oscillations in both nominal and varied mass scenarios.

**Table 7.** Performance comparison of frequency responses.

| Controllers | $T_r(s)$ | $T_s(s)$ | $OS$ (%) |
|---|---|---|---|
| HHO/PID | 2721.2 | 4843.5 | 0.0000 |
| HHO/PID | 2540 | 4520.9 | 0.0000 |
| GA/PID | 2856.7 | 5087 | 0.0000 |
| GA/PID | 2666.3 | 4747.8 | 0.0000 |
| PSO/PID | 2589 . 7 | 4611.6 | 0.0000 |
| PSO/PID | 2417.1 | 4304.1 | 0.0000 |
| HHO/FrOPID | 176.39 | 315.11 | 0.0000 |
| HHO/FrOPID | 175.46 | 313.47 | 0.0000 |
| GA/FrOPID | 178.57 | 318.22 | 0.0000 |
| GA/FrOPID | 177.66 | 316.6 | 0.0000 |
| PSO/FrOPID | 177.33 | 315.93 | 0.0000 |
| PSO/FrOPID | 176.35 | 314.17 | 0.0000 |

In summary, fractionalized-order PID controllers (FrOPID) outperform traditional PID controllers in terms of both rise time and settling time, with HHO/FrOPID being the most efficient, particularly under mass variations. This underscores the robustness and adaptability of fractional PID controllers to changes in vehicle mass.

#### *7.2.2. Effect of tire friction*

To simulate how a vehicle cruise control system is affected by tire friction, a $k_f$ friction coefficient is added, then the transfer function would be updated by adding this coefficient to the damping terms. Assuming the

damping term is $s + b$, where $b$ is the original damping, we modify this to $s + b + k_f$, where $k_f$ is the friction effect ($k_f = 0.1$). Figure 7 compares the performance of various controllers in the presence of tire friction, showing how quickly they reach steady-state after a disturbance.

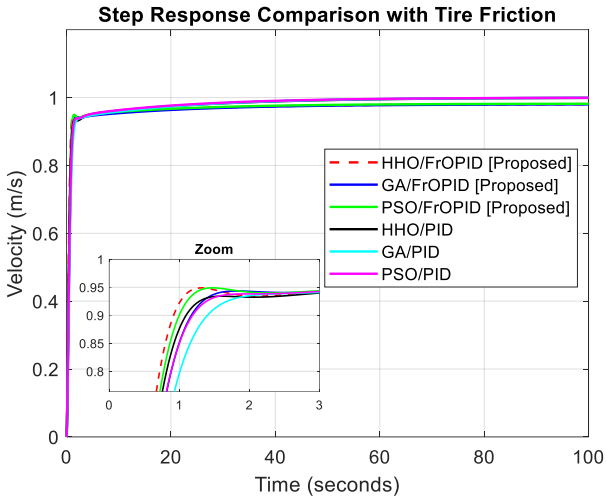


**Figure 7.** Response to tire friction.

The proposed fractional PID controllers, like HHO/FrOPID and PSO/FrOPID, respond faster than traditional PID controllers, with HHO/FrPID having the shortest rise time and PSO/FrOPID showing the quickest settling time. All controllers avoid overshoot, ensuring stability.

Table 8 presents the transient response metrics under tire friction, highlighting the performance differences between various controllers in terms of rise time, settling time, and overshoot.

**Table 8.** Performance comparison of transient responses.

| Controllers | $T_r(s)$ | $T_s(s)$ | $OS$ (%) |
|---|---|---|---|
| HHO/FrOPID | 0.72735 | 14.877 | 0.0000 |
| GA/FrOPID [Proposed] | 0.93062 | 16.448 | 0.0000 |
| PSO/FrOPID [Proposed] | 0.79483 | 14.348 | 0.0000 |
| HHO/PID | 0.9381 | 25.863 | 0.0000 |
| GA/PID | 1.2189 | 26.076 | 0.0000 |
| PSO/PID | 1.0218 | 23.78 | 0.0000 |

As can be seen from Table 8:

- **For Rise Time**: The time it takes for the system to go from 0% to 90% of the final value. The proposed HHO/FrOPID controller has the fastest rise time at 0.727 seconds, while the traditional PID controllers have longer rise times, with GA/PID controller being the slowest at 1.219 seconds.

- **For Settling Time**: The time it takes for the system to stabilize within a small range around the final value. The proposed PSO/FrOPID controller shows the shortest settling time of 14.348 seconds, with the traditional controllers settling much later, with GA/PID controller taking 26.076 seconds.

- **For Overshoot**: None of the controllers exhibit any overshoot, meaning the system does not exceed the desired value, indicating a well-damped response across all controllers.

In summary, fractional PID controllers, especially those optimized by HHO and PSO, demonstrate superior dynamic responsiveness and faster stabilization in systems with tire friction compared to traditional PID controllers.

## 8. Conclusion

This research highlights the advantages of fractional-order PID (FrOPID) controllers over conventional PID controllers in regulating the complex dynamics of vehicle cruise control systems. The FrOPID controller significantly improves flexibility and performance by incorporating an additional tuning parameter, particularly under diverse operating conditions. The study conducts a comparative analysis using three metaheuristic optimization algorithms—Harris Hawks Optimization (HHO), Genetic Algorithm (GA), and Particle Swarm Optimization (PSO)—and concludes that the HHO-optimized FrOPID offers the most effective approach, achieving an optimal balance between responsiveness and stability. These findings reinforce the effectiveness of fractional-order controllers as viable solutions for modern cruise control applications, demonstrating their capability to handle nonlinearity and unpredictability in automotive systems.

Future research will focus on empirically evaluating the proposed FrOPID methodology in real automotive systems to assess its practical effectiveness. Additionally, exploring hybrid optimization techniques to enhance the tuning process could further improve performance and reliability. Applying this framework to

other complex dynamic systems, such as robotics and industrial automation, will demonstrate the versatility of FrOPID controllers across various fields. Furthermore, integrating machine learning-based predictive models into controller design could enhance intelligence and adaptability, enabling FrOPID to be utilized in a broader range of dynamic and unpredictable scenarios.

## Competing Interest Statement

The authors declare no known competing financial interests or personal relationships that could have influenced the work reported in this paper.

## Data Availability Statement

No data or additional materials were utilized for the research described in the article.

## References

[1] Z. Nie and H. Farzaneh, "Adaptive cruise control for eco-driving based on model predictive control algorithm," *Applied Sciences*, vol. 10, no. 15, pp. 5271, 2020, https://doi.org/10.3390/app10155271.

[2] S. Chen, Q. Xiong, Y. Chen, J. Zhang, J. Yu, et al., "Eco-driving: A scientometric and bibliometric analysis," *IEEE Transactions on Intelligent Transportation Systems*, vol. 23, no. 12, pp. 22716-22736, 2022, DOI:10.1109/TITS.2022.3200588.

[3] D. Izci and S. Ekinci, "A novel hybrid ASO-NM algorithm and its application to automobile cruise control system," in *2nd International Conference on Artificial Intelligence: Advances and Applications*, Singapore, 2022, pp. 333-343, DOI: 10.1007/978-981-16-6332-1_29.

[4] K. Osman, M. F. Rahmat, and M. A. Ahmad, "Modelling and controller design for a cruise control system," in *2009 5th International Colloquium on Signal Processing & its Applications*, Kuala Lumpur, Malaysia, 2009, pp. 254-258, DOI: 10.1109/CSPA.2009.5069228.

[5] K. H. Ang, G. Chong, and Y. Li, "PID control system analysis, design, and technology," *IEEE Transactions on Control Systems Technology*, vol. 13, no. 4, pp. 559-576, 2005, DOI: 10.1109/TCST.2005.847331.

[6] G. J. Silva, A. Datta, and S. P. Bhattacharyya, *PID controllers: History, theory, tuning, and application to modern process control*. Springer Nature, 2021.

[7] Z. Ousaadi, H. Akroum, & A. Idir," Robustness enhancement of fractionalized order proportional integral controller for speed control of indirect field-oriented control induction motor," *Przegląd Elektrotechniczny*, vol. 2024, no. 3, pp. 35-40, 2024, doi:10.15199/48.2024.03.30.

[8] H. O. Bansal, R. Sharma, and P. Shreeraman, "PID controller tuning techniques: A review," *Journal of Control Engineering and Technology*, vol. 2, pp. 168-176, 2012.

[9] M. Shafiee, M. Sajadinia, A. A. Zamani, and M. Jafari, "Enhancing the transient stability of interconnected power systems by designing an adaptive fuzzy-based fractional order PID controller," *Energy Reports*, vol. 11, pp. 394-411, 2024, DOI: 10.1016/j.egyr.2023.11.058.

[10] A. Idir, L. Canale, Y. Bensafia, and K. Khettab, "Design and robust performance analysis of low-order approximation of fractional PID controller based on an IABC algorithm for an automatic voltage regulator system," *Energies*, vol. 15, no. 23, pp. 8973, 2022, DOI: 10.3390/en15238973.

[11] A. K. Mishra, P. Mishra, and H. D. Mathur, "Enhancing the performance of a deregulated nonlinear integrated power system utilizing a redox flow battery with a self-tuning fractional-order fuzzy controller," *ISA Transactions*, vol. 121, pp. 284-305, 2022, DOI: 10.1016/j.isatra.2021.04.002.

[12] A. Idir, L. Canale, S. A. Tadjer, and F. Chekired, "High order approximation of fractional PID controller based on grey wolf optimization for DC motor," in *2022 IEEE International Conference on Environment and Electrical Engineering and 2022 IEEE Industrial and Commercial Power Systems Europe (EEEIC/I&CPS Europe)*, 2022, pp. 1-6. DOI: 10.1109/EEEIC/ICPSEurope54979.2022.985 4520.

[13] L. Abualigah, S. Ekinci, D. Izci, and R. A. Zitar, "Modified Elite Opposition-Based Artificial Hummingbird Algorithm for Designing FOPID Controlled Cruise Control System," *Intelligent Automation & Soft Computing*, vol. 38, no. 2, pp. 1-20, 2023, DOI: 10.32604/iasc.2023.04 0291.

[14] Y. Bensafia, A. Idir, K. Khettab, M. S. Akhtar, and S. Zahra, "Novel robust control using a fractional adaptive PID regulator for an unstable system," *Indonesian Journal of Electrical Engineering and Informatics (IJEEI)*, vol. 10, no. 4, pp. 849-857, 2022, DOI: 10.52549/ijeei.v10i4.4034.

[15] A. Idir, Y. Bensafia, L. Canale, "Performance improvement of aircraft pitch angle control using a new reduced order fractionalized PID controller," *Asian*

*Journal of Control*, vol. 25, no. 4, pp. 2588-2603, 2023, https://doi.org/10.1002/asjc.3009.

[16] A. Idir, A. Zemmit, M. Nesri, S. Guedida, H. Akroum, and L. Canale, "PID controller design with a new method based on fractionalized integral gain for cruise control system," in Proc. IEEE Int. Conf. Environ. Electr. Eng. (EEEIC/I&CPS Europe), June 2024, pp. 1–6, DOI: 10.1109/EEEIC/ICPSEurope61470.2024.10751521

[17] A. Idir, Y. Bensafia, and L. Canale, "Influence of approximation methods on the design of the novel low-order fractionalized PID controller for aircraft system," *Journal of the Brazilian Society of Mechanical Sciences and Engineering*, vol. 46, no. 2, pp. 1-16, 2024, DOI: 10.1007/s40430-023-04627-7

[18] A. Idir, H. Akroum, S. A. Tadjer, and L. Canale, "A comparative study of integer order PID, fractionalized order PID, and fractional order PID controllers on a class of stable system," in *2023 IEEE International Conference on Environment and Electrical Engineering and 2023 IEEE Industrial and Commercial Power Systems Europe (EEEIC/I&CPS Europe)*, 2023, pp. 1-6, DOI: 10.1109/EEEIC/ICPSEurope57605.2023.10194844.

[19] M. K. Rout, D. Sain, S. K. Swain, and S. K. Mishra, "PID controller design for cruise control system using genetic algorithm," in *2016 International Conference on Electrical, Electronics, and Optimization Techniques (ICEEOT)*, Chennai, India, 2016, pp. 4170-4174, DOI: 10.1109/ICEEOT.2016.7755502

[20] D. Izci, S. Ekinci, M. Kayri, and E. Eker, "A novel improved arithmetic optimization algorithm for optimal design of PID controlled and Bode's ideal transfer function based automobile cruise control system," *Evolving Systems*, vol. 13, no. 3, pp. 453-468, 2022, DOI: 10.1007/s12530-021-09402-4

[21] S. Hlangnamthip, C. Thammarat, C. Sinsukudomchai, and D. Puangdownreong, "Optimal tuning of PIDA controller for vehicle cruise control system by modified Bat algorithm," in *2024 Joint International Conference on Digital Arts, Media and Technology with ECTI Northern Section Conference on Electrical, Electronics, Computer and Telecommunications Engineering (ECTI DAMT & NCON)*, 2024, pp. 108-111, DOI: 10.1109/ECTIDAMTN CON60518.2024.10480068.

[22] R. Pradhan and B. B. Pati, "Optimal FOPID controller for an automobile cruise control system," in *2018 International Conference on Recent Innovations in Electrical, Electronics & Communication Engineering (ICRIEECE)*, Bhubaneswar, India, 2018, pp. 1436-1440, DOI: 10.1109/ICRIEECE44171.2018.9008957.

[23] P. Gunasekaran, R. Sivasubramanian, K. Periyasamy, S. Muthusamy, O. P. Mishra, P. Ramamoorthi, and M. Geetha, "Adaptive cruise control system with fractional order ANFIS PD+ I controller: optimization and validation," *Journal of the Brazilian Society of Mechanical Sciences and Engineering*, vol. 46, no. 4, pp. 184, 2024, DOI: 10.1007/s40430-024-04699-z.

[24] A. R. Abdulnabi, "PID controller design for cruise control system using particle swarm optimization," *Iraqi Journal for Computers and Informatics (IJCI)*, vol. 43, no. 2, pp. 30–35, 2017. DOI: 10.25195/ijci.v43i2.61.

[25] D. Izci and S. Ekinci, "An efficient FOPID controller design for vehicle cruise control system using HHO algorithm," in *2021 3rd International Congress on Human-Computer Interaction, Optimization and Robotic Applications (HORA)*, 2021, pp. 1-5, DOI: 10.1109/HORA52670.2021.9461336.

[26] M. Morovatdel and A. Taraghi Osguei, "Designing a PID controller for a cruise control system using genetic algorithm," *Computational Sciences and Engineering*, 2024, https://doi.org/10.22124/cse.2024.27729.1081.

[27] G. Saravanan, C. Pazhanimuthu, B. Lalitha, M. Senthilkumar, and E. Kannan, "Red Panda Optimization Algorithm-Based PID Controller Design for Automobile Cruise Control System," in *2024 International Conference on Smart Systems for Electrical, Electronics, Communication and Computer Engineering (ICSSEECC)*, 2024, pp. 33-37, DOI: 10.1109/ICSSEECC61126.2024.10 649422.

[28] R. Pradhan, S. K. Majhi, J. K. Pradhan, and B. B. Pati, "Performance evaluation of PID controller for an automobile cruise control system using ant lion optimizer," *Engineering Journal*, vol. 21, no. 5, pp. 347-361, 2017, DOI: 10.4186/ej.2017.21.5.347.

[29] B. K. Oleiwi and L. H. Abood, "Enhanced PD controller for speed control of electric vehicle based on Gorilla Troops Algorithm," *Journal Européen des Systèmes Automatisés (JESA)*, vol. 57, no. 4, 2024, DOI: 10.18280/jesa.570414.

[30] Y. Bensafia, K. Khettab, and A. Idir, "A novel fractionalized PID controller using the sub-optimal approximation of FOTF," *Algerian Journal of Signals and Systems*, vol. 7, no. 1, pp. 21-26, 2022, DOI: 10.51485/ajss.v7i1.149.

[31] S. Guedida, B. Tabbache, K. Nounou, and A. Idir, "Reduced-order fractionalized controller for disturbance compensation based on direct torque control of DSIM with less harmonic," *ELECTRICA*, vol. 24, pp. 450-462, 2024, DOI: 10.5152/electrica.2024.23194.